Detection of Peptide-Lipid Interactions in Mixed Monolayers, Using Isotherms, Atomic Force Microscopy, and Fourier Transform Infrared Analyses

Véronique Vié,* Nicole Van Mau,† Laurent Chaloin,† Eric Lesniewska,‡ Christian Le Grimellec,* and Frédéric Heitz†

*CBS, INSERM-U414, IURC, 34093 Montpellier Cedex 5; †CRBM, CNRS-UPR 1086, 34293 Montpellier Cedex 5; and ‡Laboratoire de Physique, CNRS-URA 5027, UFR Sciences et Techniques, B.P. 400, 21011 Dijon Cedex, France

ABSTRACT To improve the understanding of the membrane uptake of an amphipathic and positively charged vector peptide, we studied the interactions of this peptide with different phospholipids, the nature of whose polar headgroups and physical states were varied. Three lipids were considered: dipalmitoylphosphatidylcholine (DPPC), dipalmitoylphosphatidylglycerol (DPPG), and dioleoylphosphatidylglycerol (DOPG). The approach was carried out by three complementary methods: compression isotherms of monolayers and atomic force microscopy observations associated with Fourier transform infrared investigations. From analysis of the compression isotherms, it was concluded that the peptide interacts with all lipids and with an expansion of the mean molecular area, implying that both components form nonideal mixtures. The expansion was larger in the case of DOPG than for DPPC and DPPG because of an α to β conformational transition with an increase in the peptide molar fraction. Atomic force microscopy observations showed that the presence of small amounts of peptide led to the appearance of bowl-like particles and that an increase in the peptide amounts generated the formation of filaments. In the case of DOPG, filaments were found at higher peptide molar fractions than already observed for DOPC because of the presence of negatively charged lipid headgroups.

INTRODUCTION

We have shown recently that a primary amphipathic peptide with the sequence Ac-M-G-L-G-L-H-L-L-V-L^{10}-A-A-A-L-Q-G-A-W-S-Q^{20}-P-K$^+$-K$^+$-K$^+$-R$^+$-K$^+$-V-Cya (where Ac and Cya are acetyl and cysteamide groups, respectively) can act as an efficient carrier facilitating the cellular uptake of drugs or oligonucleotides (Chaloin et al., 1997, 1998b). This peptide (called P1 hereafter) corresponds to the association of a signal peptide (residues 1 to 20) (Briggs and Gierasch, 1986) with a nuclear localization sequence (Kalderon et al., 1984). To improve the efficiency and, in particular, the selectivity of such vector types, it is of major importance to understand the mechanism(s) leading to the membrane crossing process. The information required for this understanding is mainly related to the interactions between the vector and the various components of biological membranes.

Therefore, we undertook a study of P1 in interaction with phospholipids. The approach is based on the analysis of the compression isotherms of mixed monolayers spread at the air-water interface, which is an appropriate method for identifying the nature of the peptide-lipid interactions. Indeed, the thermodynamic relationship between monolayer and bilayer membranes is direct, and monomolecular films at the air-water interface overcome limitations such as regulation of lipid lateral-packing density and lipid composition, which occur in bilayers (Brockman, 1999). In the work described here, this technique is associated with Fourier transform infrared (FTIR) and atomic force microscopy (AFM) analyses. FTIR gives access to the conformation of the peptide within its environment (Briggs et al., 1986), whereas AFM, which allows the observation of nanometer-sized particles, provides information on the topographical organization of the transferred monolayers (Edidin, 1997; Zasadzinski et al., 1994; Mou et al., 1996; ten Grotenhuis et al., 1996; Vié et al., 1998).

In a preliminary report, we showed that P1 interacts strongly with dioleoylphosphatidylcholine (DOPC) through hydrophobic interactions leading to an expansion of the mean molecular area (Van Mau et al., 1999). This expansion, resulting from a lipid-induced modification of the peptide organization, was accompanied by a phase separation for peptide molar fractions ranging from ~0.08 to 0.4. These conclusions arose from an analysis of the compression isotherms of mixed DOPC-peptide monolayers spread at the air-water interface. Furthermore, FTIR investigations revealed an enhancement of the β conformation of the peptide in a DOPC environment, at least for high peptide molar fractions. AFM observations carried out on transferred monolayers confirmed the results obtained by isotherm analysis and visualized the formation of mixed lipid-peptide particles. However, this study was restricted to one type of phospholipid, namely DOPC, which is neutral and in the liquid expanded state.

In the present paper we extend the above study to phospholipids for which some factors are varied: 1) the nature of their polar headgroups and 2) the nature of their fatty acid moiety and thus their physical state (liquid expanded or

Received for publication 27 May 1999 and in final form 21 October 1999.

Address reprint requests to Dr. Frederic Heitz, CRBM, CNRS-UPR 1086, 1919 route de Mende, 34293 Montpellier Cedex 5, France. Tel.: +33(0)4-67-61-33-92; Fax: +33(0)4-67-52-15-59; E-mail: fheitz@puff.crbm.cnrs-mop.fr.

0006-3495/00/02/846/11 $2.00

liquid condensed, which are designated hereafter as LE and LC, respectively). We describe the compression isotherms of spread mixed P1-phospholipid monolayers (Subramanian et al., 1986; Palmer and Thompson, 1989; Maget-Dana and Ptak, 1995; 1997; Huang and Thompson, 1996; Taneva and Keough, 1994), together with AFM observations made on the corresponding transferred films in association with a FTIR analysis.

MATERIALS AND METHODS

Materials

Dipalmitoylphosphatidylcholine (DPPC), dipalmitoylphosphatidylglycerol (DPPG), and dioleoylphosphatidylglycerol (DOPG) were purchased from Sigma Chemical Co. (St. Louis, MO). The peptide has the same origin as described in Chaloin et al. (1997), and it was synthesized by solid-phase peptide synthesis, using the Fmoc strategy, with AEDI-Expansin resin on a 9050 PepSynthesizer Milligen (Millipore). Purification was achieved by semipreparative high-performance liquid chromatography, using a Nucleosil 300, C8, 5-μm column. The peptide was identified by electrospray mass spectrometry (M_{exp} = 3014, M_{theor} = 3015.9), amino acid analysis, and NMR (Chaloin et al., 1997).

Monolayers

Compression isotherms of monolayers were recorded using a Langmuir balance setup with a 657 cm^2 trough. The surface tensions were measured with a Prolabo (Paris, France) tensiometer, by the platinum plate method of Wilhelmy. Isotherms were recorded on a XY Kipp and Zonen (Delft, the Netherlands) model BD 91 recorder. DPPC, DPPG, and DOPG solutions were prepared by dissolving the phospholipid in a chloroform/methanol mixture (5/1, v/v), and the peptide was dissolved in a minimal amount of dimethylsulfoxide (DMSO) and then diluted to a final DMSO/chloroform/methanol mixture (0.03/5/1, v/v). Lipid-peptide mixtures were prepared at the desired compositions and spread on the water, and then the solvent was allowed to evaporate for at least 10 min before the compression was started, at a rate of 0.015 nm^2/molecule/min. The differences (which can be seen in Fig. 1) for the pure peptide very probably have their origin in the fact that the peptide is poorly soluble in the chloroform/methanol mixture and that DMSO was used to enhance the solubility. Because of this behavior and the strong tendency of the peptide to precipitate, freshly prepared and different stock solutions were used for each series of measurements, which were reproduced at least five times. Therefore the analysis is valid only within each series, which deals with one type of phospholipid. For the subphase, unbuffered tridistilled water was used to create the same experimental conditions as those of the transfer (see below).

Langmuir-Blodgett monolayers

All transfers were achieved according to a procedure similar to that reported by Von Nahmen et al. (1997) and Dufrêne et al. (1997). Molecular films were formed by spreading solutions on the air-water interface on a 2-cm-deep rectangular teflon trough with an area of 70–270 cm^2. After evaporation of the solvent, the films were compressed at the above-mentioned rate up to the surface pressure required for the transfer (~36 mN/m) (Demel et al., 1975). After 10 min of relaxation, the films were transferred to the appropriate and wettable solid support (glass slides or freshly cleaved mica for AFM or a germanium crystal for FTIR) by a single crossing of the monolayer from the subphase to the air at a rate of 5 mm/min, while the surface pressure was kept constant by the use of a feedback system. Only samples for which the transfer efficiency was better than 95% were retained. The subphase was unbuffered and salt free, to avoid the presence of salt crystals on the samples.

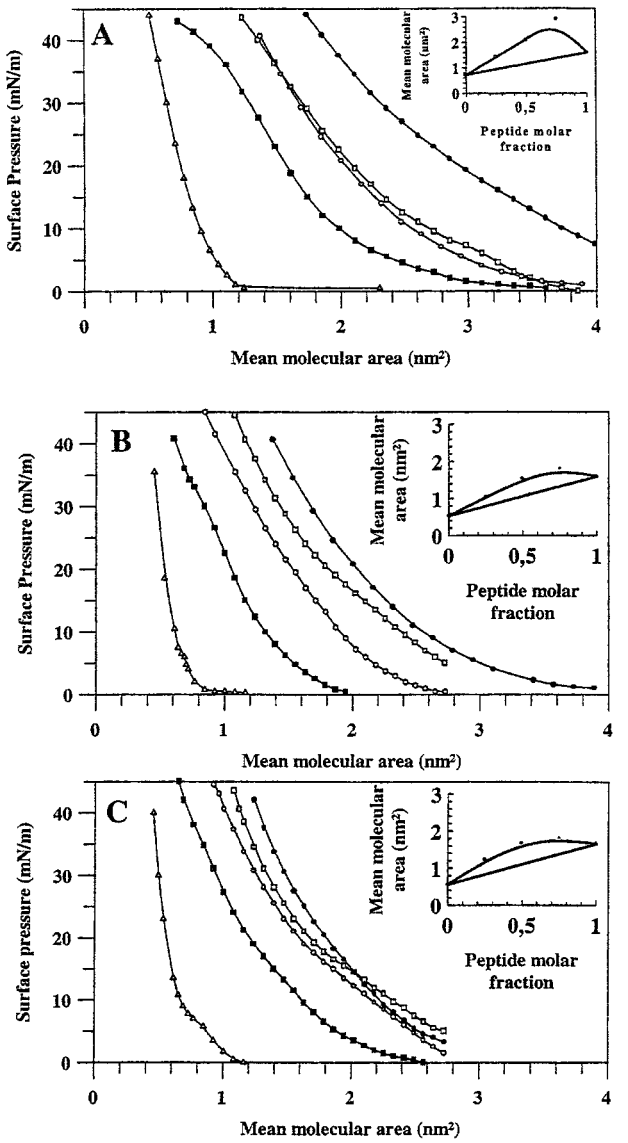

FIGURE 1 Variations of the surface pressure with the mean molecular areas of mixed lipid-P1 monolayers at various peptide molar fractions (x_p). For *A*, *B*, and *C* the lipid is DOPG, DPPG, and DPPC, respectively. For the sake of clarity, only a selected set of isotherms is shown. In *B* and *C*, the surface pressures at large molecular areas are not shown because they revealed very low pressures (<1 mN/m at 4 nm^2) and were recorded with another set of experiments dictated by the dimensions of our trough. Also note that in *B* and *C* the low pressure phase transitions of the pure lipids do not appear clearly because of the scale, which introduces a drastic smoothing of the isotherms, but they were clearly distinguishable on the experimental recordings. △, x_p = 0; ■, x_p = 0.25; □, x_p = 0.5; ●, x_p = 0.75; ○, x_p = 1. The insets show the variations, at 20 mN/m, of the mean molecular areas as a function of the peptide molar fractions.

FTIR and CD measurements

FTIR spectra were recorded on a Bruker IFS28 spectrometer equipped with a liquid nitrogen-cooled MCT detector. The spectra (1000–2000 scans)

were recorded at a spectral resolution of 4 cm^{-1} and were analyzed using the OPUS/IR2 program. They were recorded for transferred mixed monolayers and for samples that were obtained by deposition of solutions of lipid and peptide mixtures (see above) onto a fluorine plate, where the solvent was allowed to evaporate under a nitrogen stream. Complete removal of the DMSO was achieved by washing the film with water and drying under a nitrogen stream. The complex contour observed for peptidic amide I and II bands was decomposed using the second-derivative method for the determination of the band positions. All FTIR experiments were repeated at least twice on different sample preparations.

CD spectra were recorded on a Jobin-Yvon Mark V dichrograph, using quartz cells with an optical path of 1 mm. The samples were prepared by mixing a solution of P1 in water with freshly prepared DOPG vesicles obtained by sonication.

AFM observations

The topographies of the transferred monolayers were obtained using a Nanoscope III atomic force microscope from Digital Instruments (Santa Barbara, CA) working in the contact mode. Images were acquired under ambient conditions with a 14-μm piezoelectric scanner. Commercial silicon nitride cantilevers were used for the measurements. The nominal imaging force during scanning was ~0.5 nN (200-μm-long cantilever, k = 0.06 N/m). The scan rate was 2.5 Hz. Images were obtained from at least two different samples prepared on different days with at least five macroscopically separated areas on each sample.

RESULTS

Isotherms of mixed monolayers

Fig. 1 shows the isotherms of various peptide-lipid mixtures, where the lipid is DOPG, DPPG, and DPPC for Fig. 1, *A*, *B*, and *C*, respectively. The curves corresponding to the pure lipids are in agreement with those already reported (Lakhdar-Ghazal and Tocanne, 1981; Tamm and McConnell, 1985; Ruano et al., 1998). Because the collapse of the pure peptide is above 40 mN/m (54 mN/m), no collapse can occur for the mixed monolayers in the range of pressure studied here, and therefore the peptide is not squeezed out of the monolayer (Gaines, 1966). It must be noted that the isotherms are reproducible after recompression when the first compression is stopped below 20mN/m. The insets show the variations at 20 mN/m of the mean molecular area as a function of the peptide molar fraction. Whatever the lipid, a positive deviation from additivity (Crisp, 1949) can be noticed, indicating interactions within the monolayer with an expansion of the mean molecular area (Gaines, 1966; Taneva and Keough, 1994). Close examination of the insets indicates that the molecular expansion is larger for the lipid in the liquid expanded (LE) state than for those in the liquid condensed (LC) state (twofold expansion for DOPG, compared with 1.2 for DPPC and DPPG), and we note that the maximum expansion shifts toward higher peptide molar fractions on going from DOPC (x = 0.35) to DOPG (x = 0.75) (Van Mau et al., 1999). To gain better insight into the behavior under physiological conditions, some of the experiments described above are duplicated with a saline subphase. No significant difference can be detected for spread monolayers, while the influence of the presence of salt strongly modifies the peptide adsorption into a spread lipid monolayer (manuscript in preparation). Therefore, because all of the monolayer and AFM experiments are related to spread mixed monolayers, the effect of the presence of salt will not be taken into account in the discussion here.

FTIR investigations

The FTIR spectra obtained for transferred monolayers are almost identical, whatever the nature of the phospholipid and the peptide molar fraction at high x_p (0.25 or 0.50). Typical spectra are shown in Fig. 2. All spectra are characterized by the presence of an amide I band component centered at 1625 cm^{-1}, accompanied by several contributions at higher wavenumber. The 1625 cm^{-1} band identifies a β-type conformational state, and owing to the presence of a contribution in the amide I band lying at 1694 cm^{-1}, it is very likely that we are dealing with an antiparallel arrangement of the peptide chains (Dong et al., 1990; Arrondo et al., 1993). The other contributions in this wavenumber region are very probably due to vibrations of the helical and/or nonordered domains of the peptide (see below), and their absolute amplitude and assignment cannot be assessed precisely because of the low signal-to-noise ratio, especially for x_p = 0.25.

Because no information can be obtained for low peptide molar fractions with the transfer procedure because of sensitivity limits, the intensity of the amide bands is enhanced by deposition of mixed solutions onto a fluorine plate. Because of the presence of DMSO, which is a solvent that is only slightly volatile, it was of major importance to check whether it can be totally removed when the washing procedure reported in the experimental section is used. On the basis of the infrared spectrum, it can be assessed that the washing procedure is sufficient but necessary to totally eliminate the DMSO, as shown in the spectra of Fig. 3. The washing procedure also has the advantage of inducing the multilamellar organization of the lipid (Bechinger et al., 1999). The two typical behaviors induced by DOPG and DPPG are shown in Fig. 4. A zooming of the amide I and II region at three crucial values of x_p in the case of DOPG is shown in Fig. 5. In this case, it appears that an increase in x_p leads to a modification of the infrared spectrum, in both the amide I and amide II band regions. Indeed, at low x_p ($<$0.1) the major component of the amide I band is centered at 1655 cm^{-1}, and an increase in x_p induces the appearance of a contribution at 1625 cm^{-1}, which becomes the major component by a further increase in x_p. Clearly, such an evolution of the positioning of the amide I band is indicative of a conformational change of the peptide. The behavior of the amide II band, which lies around 1550 cm^{-1} at low x_p and moves to 1530 cm^{-1} at x_p = 0.5, also agrees with a conformational transition of the peptide. While the 1625 cm^{-1} amide I band in association with an amide II band at

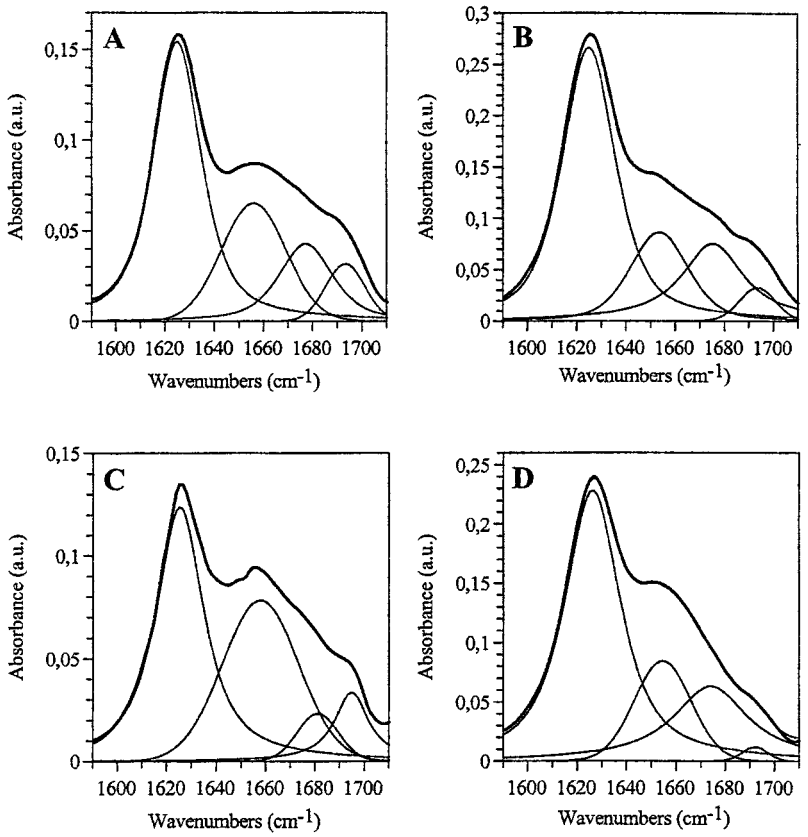

FIGURE 2 FTIR spectra in the amide I region of transferred mixed lipid-P1 monolayers at peptide molar fractions of 0.5. In *A*, *B*, *C*, and *D* the lipid is DOPC, DOPG, DPPC, and DPPG, respectively. The positions of the amide I band components were determined by the second derivative method.

1530 cm^{-1} can be unambiguously assigned to a β-type conformational state, the assignment of the low x_p conformational state is not as straightforward, although the infrared characteristics strongly suggest an α-helical conformation. Similar results were obtained using DOPC instead of DOPG, with, however, a shift of the transition toward lower values of x_p (data not shown). The existence of an α-helical structure at low x_p was confirmed by circular dichroism experiments carried out on peptide-containing DOPG vesicles (Fig. 6). The spectrum at $x_p = 0.05$ is characterized by two minima at 207 and 222 nm, with ellipticities that are nearly identical to those obtained in the presence of sodium dodecyl sulfate (SDS) micelles (Chaloin et al., 1997).

Concerning the situation found with DPPG, from infrared observations it appears that no conformational changes occur when x_p is varied, because the major amide I band contribution remains at 1625 cm^{-1}, regardless of the x_p characterizing a β-type conformation; this also holds true for DPPC.

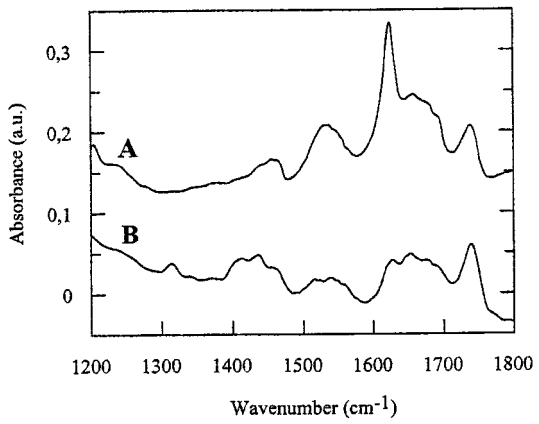

FIGURE 3 FTIR spectra of a mixed lipid-peptide sample ($x_p = 0.5$) obtained by evaporation of the solvent mixture (*B*) and after water treatment (*A*).

AFM observations

Fig. 7 shows the AFM image obtained for a transferred monolayer made of pure DOPG, which is given for reference purposes. It shows a regular and flat area, as already found for DPPG and DPPC.

Lipid in the liquid expanded state (DOPG)

A selected set of the most representative photographs obtained by AFM on peptide-containing transferred monolayers of DOPG in the liquid expanded state is shown in Fig. 8. To make significant comparisons, our attention focused on three different situations, which correspond to $x_p = 0.05$, 0.25, and 0.50.

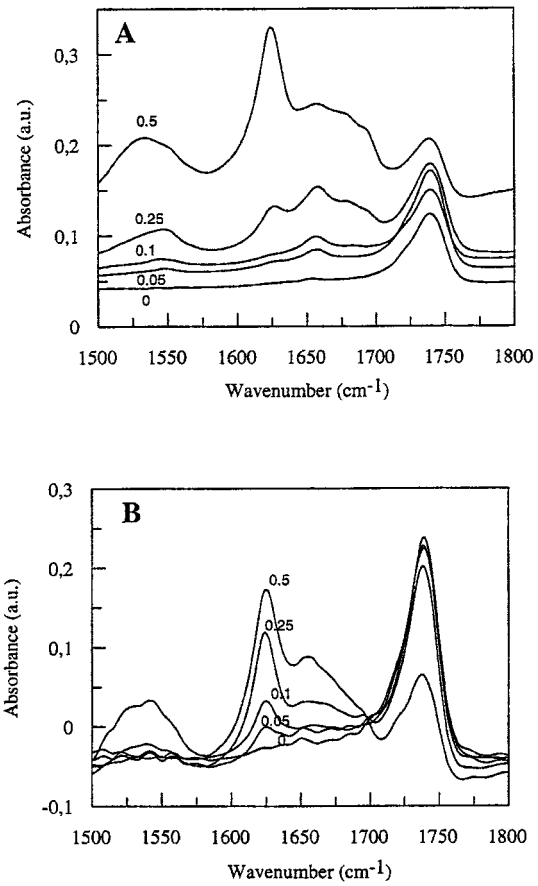

FIGURE 4 Variations of the FTIR spectra in the amide I and II bands region of mixed lipid-P1 mutilayers as a function of the peptide molar fractions. In *A* and *B* the lipids are DOPG and DPPG, respectively. The peptide molar fractions are indicated on the spectra. Note that the band centered at 1740 cm^{-1} correspond to the lipidic carbonyls. The spectra shown in this figure were recorded after water washing and drying under a nitrogen stream.

For the lowest x_p ($x_p = 0.05$) it is difficult to detect structures on the 2×2 μm scan (Fig. 8 *a*), but microheterogeneities together with round structures can be observed at higher magnification (see Fig. 8 *b*). The mean diameter of these structures was ~10 nm, and they protrude from the background from 0.5 to 0.8 nm (Fig. 9 *a*). At $x_p = 0.25$, besides the round structures described above (Fig. 8, *c* and *d*), filamentous structures (~10-nm width and 0.8-nm height) are observed (Fig. 9 *b*), together with a few rough macrodomains protruding ~3 nm from the monolayer.

When x_p is increased to 0.50, the filaments and macrodomains disappear and give way to irregular aggregates (0.7–1 nm high) (Fig. 8, *e* and *f*, and Fig. 9 *c*).

Lipids in the liquid condensed state (DPPG and DPPC)

Owing to the much lower deviation from linearity of the mean molecular area, the reported AFM observations are restricted to monolayers containing small peptide amounts ($x_p = 0.05$). In DPPG, only round micro- and macrodomains (~0.3 nm high; diameter up to 50 nm) (Fig. 9 *d*) are detected, together with small aggregates (Fig. 10, *c* and *e*). With DPPC, filaments are detected and are located between domains (Fig. 10, *d* and *f*). Such filaments are reminiscent of the situation of DOPG at $x_p = 0.25$ (see above, Fig. 8, *c* and *d*) and of that already found for DOPC (Van Mau et al., 1999). These features are also accompanied by large aggregates up to ~4 nm in height (Fig. 9 *e*) and holes in the lipid domains.

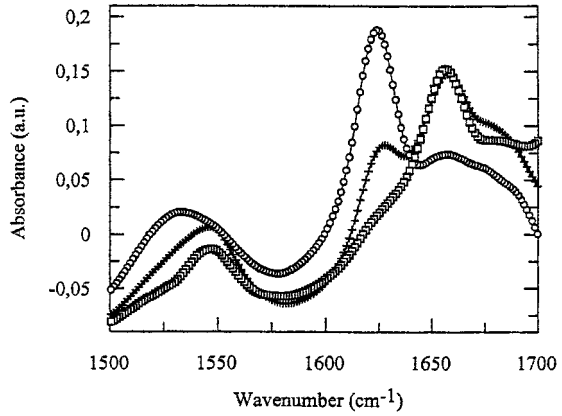

FIGURE 5 Magnification of the FTIR (normalization procedure) spectra shown on Fig. 4 *A* (amide I and II band region), at the three most significant peptide molar fractions: □, $x_p = 0.05$; +, $x_p = 0.25$; ○, $x_p = 0.5$.

DISCUSSION

From FTIR spectroscopic investigations and by comparison of the spectra shown in Figs. 2 and 4, it appears that the two procedures for sample preparation, transfer and deposition, lead to very similar spectra, at least at $x_p = 0.5$. It must be emphasized that in every situation the presence of lipid

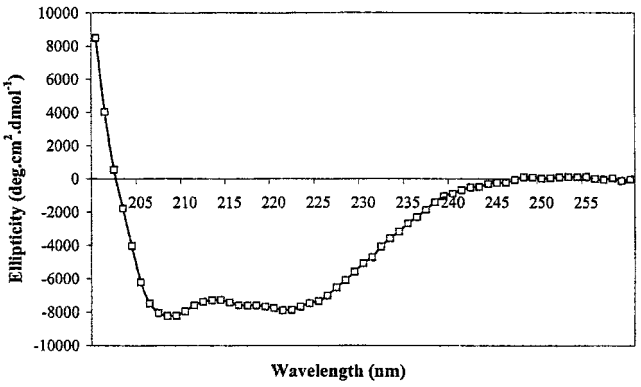

FIGURE 6 Far UV CD spectrum of P1 incorporated into vesicles of DOPG at a peptide molar fraction of 0.02.

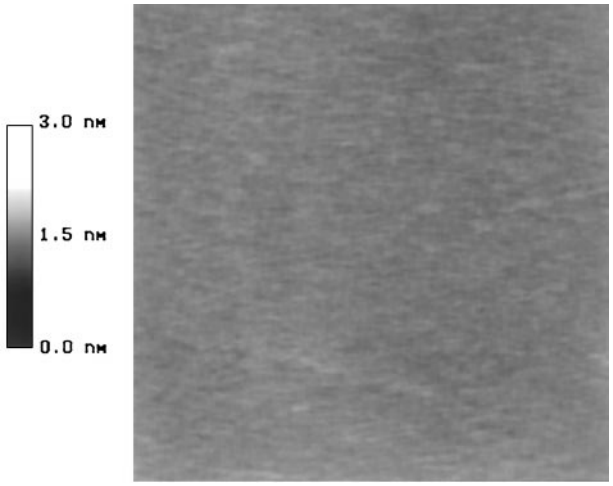

FIGURE 7 2 μm $\times$ 2 μm AFM scan of a transferred monolayer of DOPG. The height scale is given in the inset.

reduces the amount of nonordered form (see figures 4B and 7A in Van Mau et al., 1999) and that the surface pressure used for the transfer (20 or 35 mN/m) does not significantly modify the FTIR spectrum. For lower values of x_p, the spectra obtained for low pressure transferred monolayers are too noisy to allow a confident analysis. For all situations, at a high peptide molar fraction, P1 is mainly in a β-type conformational state, as revealed by the amide I band at 1625 cm^{-1}, with some part of the peptide remaining helical or nonordered, whereas for $x_p = 1$ the peptide does not adopt a well-defined conformational state and rather corresponds to a mixture of helix, random coil, and sheet structures with a strong loss of the sheet contribution (Chaloin et al. 1997). Important differences in the peptide conformation can be found at low x_p, depending on the physical state of the phospholipid. In the presence of a lipid in the LC state, no conformational transition could be detected for any value of x_p, and the peptide remains in a β-form. In the case of a lipid in the LE state, a decrease in x_p induces a $\beta \rightarrow \alpha$ conformational transition. As expected because of the influence of the charges, with DOPC this transition occurs at a lower x_p than it does with DOPG. Because of the strong similarity between the CD spectra in DOPG and SDS micelles, it can be stated that P1 adopts the same α-helical conformational state in both of these media. The helix covers the hydrophobic signal peptide sequence (from residue 1 up to 18), as revealed by NMR in SDS micelles, while the remainder of the peptide is nonstructured (Chaloin et al., 1997). It is likely that when in the β-form, the structured domain of P1 corresponds to the same hydrophobic sequence. Because of the primary amphipathic profile of the peptide and the fact that a much larger deviation from linearity occurs for DOPG than for DPPG (where no helix-to-sheet conformational transition is detectable, although they are treated identically), it seems reasonable to assume that the FTIR observations made on multilayers reflect the behavior occurring in monolayers. This is enforced by the AFM observations, which show, at low x_p, the presence of small particles protruding 0.5–0.8 nm from the hydrophobic side of transferred monolayers. These protrusions are consistent with the dimensions expected for an α-helical form oriented perpendicular to the interface (see below).

Examination of the compression isotherms reveals for every situation a positive deviation from the linearity expected, assuming an ideal miscibility without conformational changes of the peptide. Let us first consider the case where the peptide undergoes a conformational transition, i.e., with lipids in the LE state. This situation clearly occurs for DOPG, where a large deviation from linearity occurs. It must be noted that the large deviation, which can be observed at 20 mN/m (see Fig. 1 *A*), still occurs at every surface pressure and more especially at higher surface pressures. For example, at 35 mN/m (the pressure corresponding to that used for the transfer) and at $x_p = 0.75$, where the peptide is the most homogeneous from the structural point of view, the experimental molecular area is 1.6-fold that expected when an ideal is assumed (i.e., a linear behavior). Therefore, assuming that the molecular area of the lipid is not significantly affected by its mixing with the peptide, the increase in the mean molecular area agrees with the conformational change of the peptide when accompanied by a modification of its orientation. Indeed, examination of the theoretical dimensions of the various possible conformational states indicates that for an α-helix that has its helical axis perpendicular to the interface and assuming an average helical diameter of 1.5 nm, the molecular area is 1.77 nm^2 $\{\pi \times 0.75 \text{ (helix radius)}^2\}$. For the same helix, but with its axis parallel to the interface and taking into account only the 18-residue-long structured domain, the corresponding molecular area is 4.05 nm^2 (18 (number of residues) $\times$ 1.5 (helix diameter) $\times$ 0.15 (height per residue)), and 3 nm^2 when in the β-form with the peptide axis parallel to the interface (18 (number of residues) $\times$ 0.475 (interchain distance) $\times$ 0.35 (length per residue)). Because the ratio between the area of the β-form and that of the perpendicular α-helix is very close to the molecular area expansion (compare 1.7 with the experimental value of 1.6), it seems reasonable to attribute the large molecular area expansion mainly to the lipid-induced conformational changes accompanied by a modification of the peptide positioning with respect to the monolayer, with a rocking of the peptide axis from perpendicular to parallel to the interface. As for the positioning of the α-helical form, the height of the protrusions observed in the AFM images at low x_p is in line with a hydrophobic α-helix embedded in the lipid medium. A length of 18 $\times$ 0.15 = 2.7 nm is too large to span a monolayer and thus will protrude $\sim$0.7 nm, but can easily accommodate a bilayer, as suggested by the ability of this peptide to induce the formation of ionic channels in artificial bilayers (Chaloin et al., 1998a).

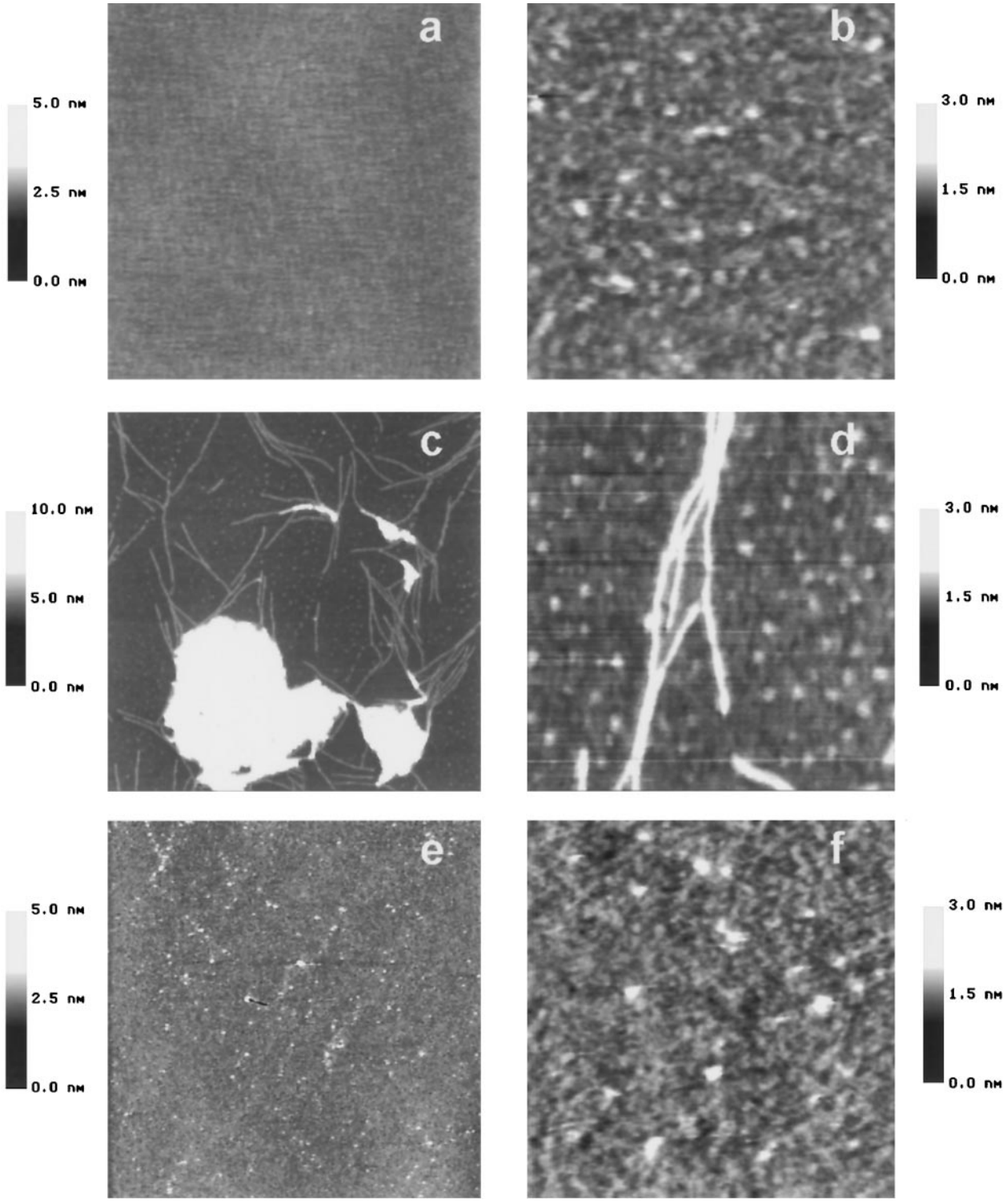

FIGURE 8 AFM scans of transferred monolayers of DOPG corresponding to $x_p = 0.05$ (*a* and *b*), 0.25 (*c* and *d*), and 0.50 (*e* and *f*). The scales are 2 μm $\times$ 2 μm for *a*, *c*, and *e* and 500 nm $\times$ 500 nm for *b*, *d*, and *f*. The height scales are given in the insets.

Concerning the shift toward higher molar fractions of the maximum of expansion (compare 0.35 for DOPC with 0.75 for DOPG), because the two lipids are differently charged, its origin probably lies in the nature of the lipid headgroups. Recalling that the peptide contains five positively charged residues that are all located at the nonstructured C-terminus

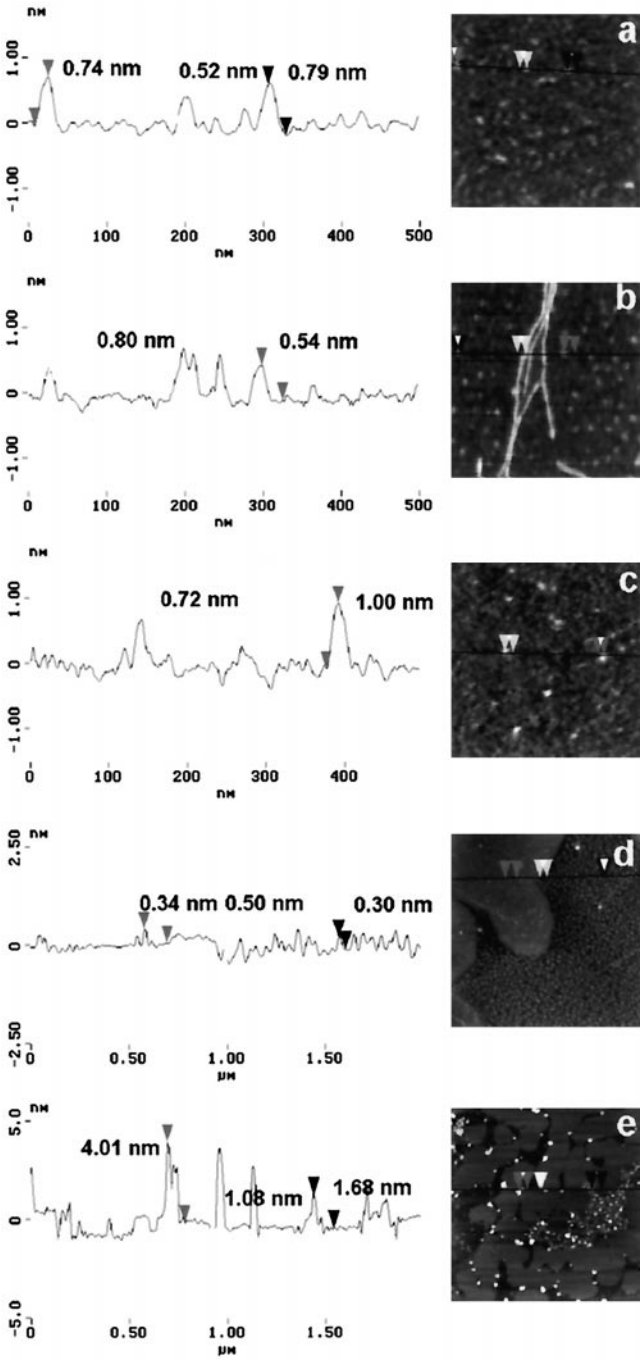

FIGURE 9 Section analysis of monolayers. The heights of the structures imaged were estimated from AFM images, using the section analysis software provided by Digital Instruments. *a*, *b*, and *c* correspond to DOPG-P1 mixtures (Fig. 8, *b*, *d*, and *f*, respectively); *d* and *e* correspond to DPPG-P1 and DPPC-P1 mixtures (Fig. 10, *c* and *d*, respectively). Note that except for aggregates in *e*, these heights are significantly lower than the thickness of a pure phospholipid monolayer.

of P1, it is likely that they can interact with the negative headgroups of DOPG. Therefore, the finding of a situation similar to that occurring with DOPC can only occur at a peptide molar fraction above that which corresponds to electroneutralization, i.e., 0.2. Below this molar fraction the attractive electrostatic interactions will favor lipid-peptide interactions and thus inhibit peptide-peptide interactions. In DOPC, the shift toward lower x_p of the α-to-β transition observed in the infrared investigations agrees with the above conclusion—a greater dispersion of the peptide, which will favor the α-helical form.

For lipids in the LC state, the deviation from linearity of the mean molecular area when x_p is varied also reflects a nonideal miscibility between the two components. However, in the work presented here, the deviation is lower than that found for lipids in the liquid expanded state. Since no α-to-β conformational transition could be detected, our results indicate that the hetero interactions are weaker than those arising in the lipids in the LE state. In addition, no major difference can be noted with modification of the charge of the lipid, indicating that in DPPC and DPPG, the general trend is governed by the physical state of the lipid.

The above conclusions can be summarized as follows. In the case of DPPC and DPPG, the deviation from linearity of the mean molecular area is induced essentially by the interactions between the components of the monolayer, while for DOPG and for DOPC, this expansion has two origins: the interactions between the components and the conformational transition of the peptide. The difference between LE and LC lipids reflects the contribution of the conformational changes.

These conclusions are corroborated by the AFM observations, which will also provide more precise insight into the nature of the structures formed when P1 is mixed with various lipids. While the presence of P1 induces phase separation in the case of DOPC (Van Mau et al., 1999), no such phenomenon can be detected with DOPG, and no domain is found in DOPG, regardless of the value of x_p (see Fig. 8). The formation of domains was assumed to be a consequence of strong hydrophobic peptide-peptide interactions in DOPC monolayers (Van Mau et al., 1999). These interactions are less favored in the case of DOPG because of the attractive electrostatic interactions between the two partners. This will favor the dispersion of the peptide in the monolayer and therefore the formation of the α-helical form. The filaments that can be observed with DOPG at high x_p are in agreement with the finding of a β-type conformation and shed some light on the size of the particles formed.

When the lipids are in the LC state (DPPC and DPPG), the general features of the AFM images reveal the existence of domains that are round for DPPG. For DPPC these domains are angular and are connected by filaments very similar to these found for DOPC.

It is likely that the differences in shapes do not have their origin in artifacts generated by the transfer. Indeed, it was shown that the transfer properties of monolayers strongly depend on the surface pressure of the monolayer (Egusa et al., 1990) and that this phenomenon is very sensitive at low

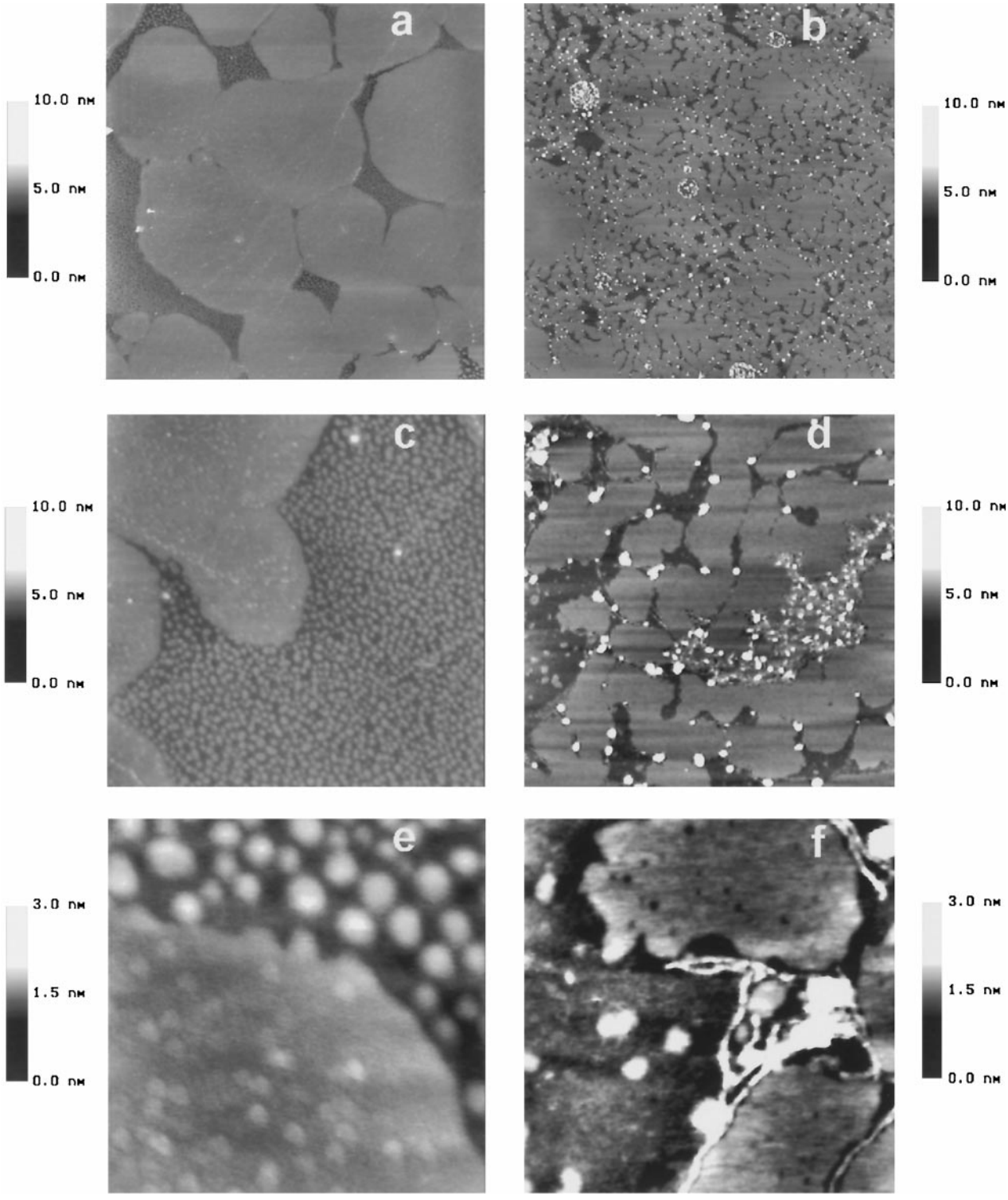

FIGURE 10 AFM scans of transferred monolayers corresponding to $x_p = 0.05$ for DPPG (*a, c,* and *e*) and DPPC (*b, d,* and *f*), respectively. Scan sizes are 8 μm $\times$ 8 μm (*a* and *b*), 2 μm $\times$ 2 μm (*c* and *d*) and 400 nm $\times$ 400 nm (*e* and *f*). The height scales are given in the insets.

surface pressures. However, when transfer takes place at high surface pressures, as done in this work, this effect is minimized (Rana et al., 1994) and thus can be neglected (Dufrêne et al., 1997; Lee et al., 1998). The absence of artifacts is also strongly supported by the continuous and reproducible evolution of the images, especially with regard

to the peptide-containing domains. It must also be noted that the AFM images do not depend on the nature of the support; i.e., glass slides or mica.

CONCLUSION

The present study used three complementary methods to show that the primary amphipathic peptide P1 interacts strongly with DOPG, which is in the LE state. An increase in x_p generates the formation of filaments, where the peptide adopts a β-type conformational state. The large expansion of the mean molecular area observed arises from peptide structuralization and/or conformational changes together with the nonideal miscibility between the peptide and the lipid. For the lipids in the LC state, the smaller domains of DPPG compared to those of DPPC are indicative of a better miscibility due to electrostatic interactions.

All of the above conclusions shed some light on the influence of the nature of the lipids composing membranes on the uptake of primary amphipathic peptides. When P1 is used as a covalent vector, the nature (ionic or not) of the linked drug will also affect the uptake because it can strongly modify the electrostatic interactions. All of this information has to be taken into account to improve the understanding of the in vivo uptake of these types of peptides because natural membranes either contain or are in the presence of ions or compounds that can strongly modify their properties, especially from the point of view of phase separation and electrostatic interactions. Because the peptide used throughout this work can act as a vector facilitating the cellular uptake of a drug (Chaloin et al., 1997) or nucleic acids (Chaloin et al., 1998), this information is also crucial for the future design of new vectors that will act in a cell-dependent manner according to the composition of the cellular membranes.

This work was supported by the GDR Peptides et Protéines Membranotropes from the CNRS and by grants from La Fondation pour la Recherche Médicale, l'Association pour la Recherche sur le Cancer, the Région Languedoc-Roussillon, and the Université de Montpellier I. L.C. was supported by a grant from the Agence Nationale de Recherche contre le SIDA. We thank also Dr. P. Bello for manuscript corrections.

REFERENCES

Arrondo, J. L. R., A. Muga, J. Castresana, and F. M. Goñi. 1993. Quantitative studies of the structure of protein in solution by Fourier-transform infrared spectroscopy. *Prog. Biophys. Mol. Biol.* 59:23–56.

Bechinger, B., J.-M. Ruysschaert, and E. Goormaghtigh. 1999. Membrane helix orientation from linear dichroism and infrared attenuated total reflection spectra. *Biophys. J.* 76:552–563.

Briggs, M. S., and L. M. Gierasch. 1986. Molecular mechanisms of protein secretion: the role of the signal sequence. *Adv. Protein Chem.* 38: 109–180.

Brockman, H. 1999. Lipid monolayers: why use half a membrane to characterize protein-membrane interactions? *Curr. Opin. Struct. Biol.* 9:438–443.

Chaloin, L., P. Vidal, A. Heitz, N. Van Mau, J. Méry, G. Divita, and F. Heitz. 1997. Conformations of primary amphipathic carrier peptides in membrane mimicking environments. *Biochemistry.* 36:11179–11187.

Chaloin, L., E. Dé, P. Charnet, G. Molle, and F. Heitz. 1998a. Ionic channels formed by a primary amphipathic peptide containing a signal peptide and a nuclear localization sequence. *Biochim. Biophys. Acta.* 1375:52–60.

Chaloin, L., P. Vidal, P. Lory, J. Méry, N. Lautredou, G. Divita, and F. Heitz. 1998b. Design of carrier peptide-oligonucleotide conjugates with rapid membrane translocation and nuclear localization properties. *Biochem. Biophys. Res. Commun.* 243:601–608.

Crisp, D. J. 1949. A two dimensional phase rule. I. Derivation of a two-dimensional phase rule for planar interface. II. Some applications of a two dimensional phase rule for a single surface. *In* Surface Chemistry. Butterworths, London. 17–35.

Demel, R. A., W. S. Geurts van Kessel, R. F. Zwaal, B. Roelofsen, and L. L. van Deenen. 1975. Relation between various phospholipase actions on human red cell membranes and the interfacial phospholipid pressure in monolayers. *Biochim. Biophys. Acta.* 406:97–107.

Dong, A., P. Huang, and W. S. Caughey. 1990. Protein secondary structure in water from second-derivative amide I infrared spectra. *Biochemistry.* 29:3303–3308.

Dufrêne, Y. F., W. R. Barger, J.-B. D. Green, and G. U. Lee. 1997. Nanometer-scale surface properties of mixed phospholipid monolayers and bilayers. *Langmuir.* 13:4779–4784.

Edidin, M. 1997. Lipid microdomains in cell surface membranes. *Curr. Opin. Struct. Biol.* 7:528–532.

Egusa, S., N. Gemma, and M. Azuma. 1990. Experimental analysis of the thermodynamic mechanism of Langmuir-Blodgett film transfer. *J. Phys. Chem.* 94:2512–2518.

Gaines, G. L. 1966. Mixed monolayers. *In* Insoluble Monolayers at Liquid-Gas Interfaces. Prigogine, editor. Interscience, New York. 281–300.

Huang, Z., and N. L. Thompson. 1996. Imaging fluorescence correlation spectroscopy: nonuniform IgE distributions on planar membranes. *Biophys. J.* 70:2001–2007.

Kalderon, D., W. D. Richardson, A. F. Markham, and A. E. Smith. 1984. Sequence requirements for nuclear localization of simian virus 40 large-T antigen. *Nature.* 311:33–38.

Lakhdar-Ghazal, F., and J. F. Tocanne. 1981. Phase behaviour in monolayer and in water dispersions of mixtures of dimannosyldiacylglycerol with phosphatidyglycerol. *Biochim. Biophys. Acta.* 644:284–294.

Lee, K. Y. C., M. M. Lipp, D. Y. Takamoto, E. Ter-Ovanesyan, and J. A. Zasadzinski. 1998. Apparatus for the continuous monitoring of surface morphology via fluorescence microscopy during monolayer transfer to substrates. *Langmuir.* 14:2567–2572

Maget-Dana, R., and M. Ptak. 1995. Interactions of surfactin with membrane models. *Biophys. J.* 68:1937–1943.

Maget-Dana, R., and M. Ptak. 1997. Penetration of the insect defensin A into phospholipid monolayers and formation of defensin A-lipid complexes. *Biophys. J.* 73:2527–2533.

Mou, J., D. M. Czalkowsky, and Z. Shao. 1996. Gramicidin A aggregation in supported gel state phosphatidylcholine bilayers. *Biochemistry*. 35: 3222–3226.

Palmer, A. G., and N. L. Thompson. 1989. Fluorescence correlation spectroscopy for detecting submicroscopic clusters of fluorescent molecules in membranes. *Chem. Phys. Lipid.* 50:253–270.

Rana, F. R., S. W. Widayati, B. W. Gregory, and R. A. Dluhy. 1994. Metastability in monolayer films transferred onto solid substrates by the Langmuir-Blodgett method: IR evidence for transfer-induced phase transitions. *Appl. Spectrosc.* 48:1196–1203.

Ruano, M. L., K. Nag, L.-A. Worthman, C. Casals, J. Pérez-Gil, and K. M. W. Keough. 1998. Differential partitioning of pulmonary surfactant protein SP-A into regions of monolayers of dipalmitoylphosphatidylcholine and dipalmitoylphosphatidylcholine/dipalmitoylphosphatidylglycerol. *Biophys. J.* 74:1101–1109.

Subramanian, S., M. Seul, and H. M. McConnell. 1986. Lateral diffusion of specific antibodies bound to lipid monolayers on alkylated substrates. *Proc. Natl. Acad. Sci. USA.* 83:1169–1173.

Tamm, L. K., and H. M. McConnell. 1985. Supported phospholipid bilayers. *Biophys. J.* 47:105–113.

Taneva, S., and K. M. W. Keough. 1994. Pulmonary surfactant proteins SP-B and SP-C in spread monolayers at the air-water interface. I. Monolayers of pulmonary surfactant protein SP-B and phospholipids. *Biophys. J.* 66:1137–1148.

ten Grotenhuis, E., R. A. Demel, M. Ponec, D. R. Boer, J. C. Miltenburg, and J. A. Bouwstra.1996. Phase behavior of stratum corneum lipids in mixed Langmuir-Blodgett monolayers. *Biophys. J.* 71:1389–1399.

Van Mau, N., V. Vié, L. Chaloin, E. Lesniewska, F. Heitz, and C. LeGrimellec. 1999. Lipid induced organization of a primary amphipathic peptide: a coupled AFM-monolayer study. *J. Membr. Biol.* 167: 241–249.

Vié, V., N. Van Mau, E. Lesniewska, J. P. Goudonnet, F. Heitz, and C. Le Grimellec. 1998. Distribution of ganglioside G_{M1} between two-components, two-phase phosphatidylcholine monolayers. *Langmuir*. 14: 4574–4583.

Von Nahmen, A., M. Schenk, M., Sieber, and M. Amrein. 1997. The structure of a model pulmonary surfactant as revealed by scanning force microscopy. *Biophys. J.* 72:463–469.

Zasadzinski, J. A., R. Viswanathan, L. Madsen, J. Gaenaes, and D. K. Schwartz. 1994. Langmuir–Blodgett films. *Science*. 263:1726–1733.